reprecipitation to the remaining droplets during subsequent cooling; or coagulation due to droplet collisions induced by Marangoni convection.

We will first test the hypothesis of convection-induced coagulation. The velocity, v, of a particle of radius r is given by

$$v = -\frac{2}{3}\frac{r}{2\eta_1 + 3\eta_2}\frac{d\sigma}{dT}\frac{dT}{dy} \quad (1)$$

where η_1 is the viscosity of the zinc matrix and η_2 is the viscosity of the lead droplets. The temperature coefficient of surface tension, $d\sigma/dT$, is of the order of 0.1 mJ/m^2-K between L_1 and L_2 in a miscibility gap system (*6*). Assuming a temperature gradient, dT/dy, of the order of magnitude of 1 K per centimeter, we obtain velocities between 0.1 and 2 μm/sec for particle sizes from 1 to 20 μm. These particle velocities are about two orders of magnitude smaller than those tested in earlier terrestrial experiments, which could be shown to make a negligible contribution to particle coarsening (*3*).

For Ostwald ripening, the LSW theory (*4, 5*) predicts the following relation between mean particle radius and time:

$$\bar{r}(t)^3 - \bar{r}(0)^3 = kt \quad (2)$$

$$k = \frac{8\sigma C_0 D\Omega^2}{9RT} \quad (3)$$

The boundary energy, σ, between the liquid lead-rich particles and the zinc-rich melt is about 100 mJ/m^2 (*7*); the solubility, C_0, of lead in molten zinc is 2 percent by weight at 480°C (see Fig. 1); the molar volume, Ω, of lead is 18 cm^3/mole; and the gas constant, R, is 8.3 J/mole-K. The rate constant, k, of Ostwald ripening calculated from the mean particle radius before and after flight is 0.035 μm^3/sec, which would yield a diffusion coefficient for lead in liquid zinc at 480°C of 10^{-4} cm^2/sec. This result is in agreement with a value for the diffusion of lead in liquid zinc in a 1-*g* experiment by Pelzel [$D_{500°C} = 3 \times 10^{-4}$ cm^2/sec (*8*)], but is about 30 times larger than values that were obtained in our terrestrial Ostwald ripening experiments (*9*). While Pelzel's data may have been high because of convection, ours may have been low because of loss of large particles by sedimentation. In view of the lack of diffusivity measurements unaffected by gravity, we can only note that the diffusivity calculated from our Spacelab experiment is within the range spanned by available data.

The discussion above shows that Ostwald ripening would be a plausible mechanism for the observed increase in droplet size. However, the effect of precipitation on the droplets during cooling from the hold temperature has to be analyzed more accurately before final conclusions can be drawn. For this, the number of droplets per unit volume must be determined from an accurate size distribution analysis, and this will be among the next steps in the evaluation of our Spacelab results.

ALBERT KNEISSL
Institut für Metallkunde und Werkstoffprüfung, Montanuniversität A-8700 Leoben, Austria
HELLMUT FISCHMEISTER
Max-Planck-Institut für Metallforschung, D-7000 Stuttgart 80, Federal Republic of Germany

References and Notes

1. L. L. Lacy and G. H. Otto, AIAA paper No. 74-1242 (New York, 1975).
2. C. Y. Ang and L. L. Lacy, *ASTP Experiment MA-044, NASA TMX-64956* (Marshall Space Flight Center, Huntsville, Ala., 1975).
3. A. Kneissl, R. Pfefferkorn, H. Fischmeister, in *Proceedings of the 4th European Symposium on Materials Sciences under Microgravity, Madrid* (ESA SP-191, European Space Agency, Paris, 1983), p. 55.
4. I. M. Lifshitz and V. V. Slyozov, *J. Phys. Chem. Solids* **19**, 35 (1961).
5. C. Wagner, *Z. Elektrochem.* **65**, 581 (1961).
6. H. Fredriksson, in *Proceedings of a Workshop on the Effect of Gravity on Solidification of Immiscible Alloys, Stockholm* (ESA SP-219, European Space Agency, Paris, 1984).
7. R. Pfefferkorn, thesis, Montanuniversität Leoben, Leoben, Austria (1981).
8. E. Pelzel, *Z. Metallkd.* **61**, 289 (1970).
9. A. Kneissl and H. Fischmeister, *Metall (Berlin)* **37**, 131 (1983).
10. Financial support by the Austrian Ministry of Science and Research is gratefully acknowledged.

27 March 1984; accepted 30 May 1984

Unidirectional Solidification of Cast Iron

Abstract. *The segregation of sulfur in liquid cast iron was studied under conditions of microgravity on Spacelab 1. A rod of cast iron containing carbon, silicon, sulfur, and phosphorus was unidirectionally solidified at four different rates. The influence of sulfur on the graphite structure and the stability of an aluminum oxide skin deposited on the surface of the specimen were investigated.*

On day 4 of the Spacelab 1 mission experiment 1ES325 was conducted as planned. Liquid cast iron containing 3.9 percent carbon, 1.5 percent silicon, 0.025 percent sulfur, and 0.01 percent phosphorus was unidirectionally solidified at four different rates varying between 0.1 and 1 mm/min (*1*). Before the successful run of the experiment a problem occurred with the temperature control of the isothermal heating furnace (IHF) with gradient device after it had been preheated. After the furnace had been cooled down, the experiment was restarted by the payload specialists.

Analysis. The specimen as received from Spacelab after the mission was examined by different techniques. It consisted of a cast iron rod 139 mm long contained in a crucible. An Al_2O_3 skin was deposited on the surface of the specimen (*2*). The examination proceeded from the outside to the inside. First, x-rays were used to determine the location and position of the cast iron within the crucible. In addition, the condition of Pt-PtRh10 thermocouples mounted at the surface of the rod within the crucible was established.

The crucible was then removed with a rapidly rotating diamond saw, which made two cuts along the length of the crucible with a depth equal to the thickness of the crucible. After removal of the crucible, the Al_2O_3 skin was examined by light optical microscopy and scanning electron microscopy combined with x-ray energy-dispersive analysis. From this, information was obtained on the morphology and chemical composition of the skin.

Then the rotating diamond saw was used to cut the sample over its whole length into two parts. For this purpose the sample was moved along the cutting wheel with a speed of about 0.5 mm/min.

After grinding on silicon carbide abrasive paper and polishing on diamond with particle sizes of 3, 1, and 0.25 μm, together with intermittent weak nital etching, the graphite structure was studied with a light optical microscope.

Results and discussion. The x-ray photography showed that the liquid column of the specimen had been separated into two parts, which were 85 mm and 26 mm in length. Two effects may have played a role in this separation. The highest temperature in the IHF was in a confined region near the end of the rod. This caused the material to start melting in a radial direction at some distance from the outer end of the rod. Unlike most metals, gray cast iron shrinks during melting. Because of this shrinkage and the surface tension, the first melted zone had a tendency to break into two parts under microgravity conditions. Furthermore, the unexpected development of some gases may have caused the smaller part to be pushed toward the end of the crucible as some pressure built up. This effect could also explain why some of the molten iron may have been pushed

out of the crucible through one of the holes in its end cap. These holes were used to evacuate the space within the crucible.

Apart from the separation of the liquid column, a cavity was observed at a distance of 22 mm from the specimen holder. This will be discussed at the end of this section.

Investigations of the Al_2O_3 skin showed that it was rigid enough to keep the liquid specimen in its original shape, although a number of cracks could be observed. At the location where the smaller part of the cast iron had been pushed toward the end of the crucible and where material was missing, the skin was still in place. The skin collapsed only at two small regions at the ends of the grooves in which the thermocouples were lying. At the "cold" side of the rod, where the cast iron had not been melted, the Al_2O_3 skin contained some microcracks. The structure of the skin at this end—where the temperature did not exceed 800°C—remained amorphous. Crystallization occurred at places where the temperature became higher. At the "hot" end of the rod—where the temperature was 1500°C during the whole experiment, about 2.5 hours—coalescence of the crystallites occurred. Whiskers were observed at some isolated regions of the skin. X-ray energy-dispersive analysis showed that they consisted of Al_2O_3 and that they had the same composition as the skin. No difference in composition was found between the amorphous and crystalline areas of the skin. No silicon could be found.

A marked phenomenon was the appearance of a large amount of small droplets of cast iron. These occurred at several isolated spots on the outer surface of the skin and on the whole inner surface of the skin in the region where the smaller part of the cast iron had been pushed away. This can be seen in Fig. 1. These spherical droplets varied in size between 1 and 4 μm. It is not clear how these droplets formed. They may have condensed from the vapor phase onto the surface of the skin during the cooling period of the experiment. Apart from these small droplets, a few relatively large droplets varying in size between 0.1 and 0.7 mm were found on the outer surface of the skin. We believe that they solidified from "floating" liquid which had leaked to regions up to 2.5 cm from the outer end of the skin. There is no evidence that they were pushed from the inside through cracks or microscopic openings at the spot where they were found.

No chemical reaction seemed to have taken place at the interface between the skin and the cast iron. Nucleation of graphite flakes at this interface was observed.

The program followed during the unidirectional solidification of the cast iron rod consisted of a heating period, a period during which the furnace plus gradient insert moved with four different speeds—0.1, 0.4, 0.7, and 1.0 mm/min for 130, 30, 18, and 12 minutes, respectively—and a cooling period (*1*). After cutting the sample into two halves it could be established that the four regions of different solidification rate did not have the length and position that would be expected on the basis of the programmed parameters. For instance, the solid-liquid interface, where the solidification started, was 10 mm closer to the specimen holder than had been expected.

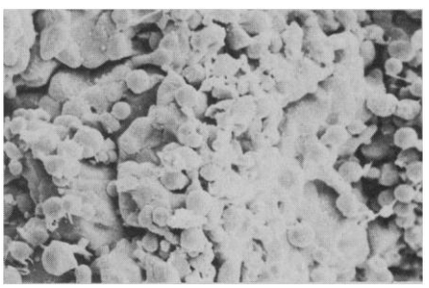

Fig. 1. Small droplets of iron on the inner surface of the Al_2O_3 skin. The visible area is 30 by 35 μm.

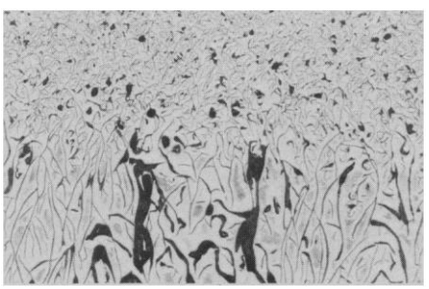

Fig. 2. Cavities at the position where the melting (from right to left) stopped and the directional solidification (from left to right) started. The largest dimension of the big cavity is 2.5 mm.

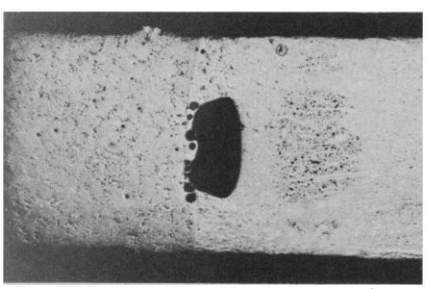

Fig. 3. Graphite structure at the transition from a solidification rate of 0.1 to a rate of 0.4 mm/min. The direction of solidification is perpendicular to the interface. The visible area is 1.8 by 2.3 mm.

Cavities were found at this starting point, which was the same place where the final melting interface stopped. The cavities consisted of a large one 2.5 mm wide and several small ones between 0.02 and 0.2 mm in size (Fig. 2). These cavities were transported through the specimen by the solid-liquid interface during melting. Two possible explanations can be given for the nucleation of the cavities. They may have formed at the progressing melting interface itself, which is the place where shrinkage of the gray cast iron takes place. (The cavities would have been filled immediately by liquid iron in ground experiments.) Or they may have formed during the first run of the experiment, which failed because of a defect in the furnace temperature indicator.

During the relatively fast cooling after the failure of the first run, parts of the specimen may have solidified as white cast iron, containing some cavities originating from shrinkage during solidification. During the second successful run of the experiment these cavities may have been swept through the rod by the melting interface. Efforts are being made to investigate these phenomena more closely in additional ground experiments.

The graphite structure in the region where the cast iron solidified at the lowest speed consisted of very coarse flakes, with an interlamellar distance of 40 μm (Fig. 3). At the next higher solidification rate a finer flake structure was observed with an interlamellar distance of 18 μm (Fig. 3). This structure did not change significantly when solidification took place at rates of 0.7 and 1.0 mm/min, in contrast to what was observed in ground experiments, where the flake distance decreased further at higher solidification rates.

One of the reasons why the size of the graphite flakes did not decrease at higher solidification rates is the fact that sulfur was accumulating at the liquid-solid interface. When the sulfur concentration increases the flakes become coarse. Because part of the rod had been separated from the rest, an even larger amount of sulfur would accumulate at the end of the larger part of the rod. In the polished sample this sulfur, which segregated as iron sulfide, could be observed with an optical microscope.

Differences in the sulfur distribution between the specimen from Spacelab 1 and specimens used in ground experi-

ments could also have been the cause of the higher density of primary dendrites in the latter specimens. In the specimen from Spacelab 1 only a few dendrites were observed in the regions with the three lowest solidification rates. At the highest rate, the number of primary dendrites was greater.

Follow-up analysis. The next analysis to be conducted will consist of measuring the sulfur, silicon, and phosphorus concentrations in the specimen. The results will be quantitatively combined with and related to those reported above, the measured temperatures and temperature gradient, and the rates of solidification (*3*).

Conclusions. The experiment on Spacelab 1 proceeded essentially as planned, but a number of unexpected phenomena occurred. The liquid metal column separated into two parts. Cavities were found at the ultimate position of the melting interface, which was closer to the specimen holder than programmed. Droplets of iron were observed on the surface of the Al_2O_3 skin. This 50-μm-thick skin was rigid enough to keep the cast iron in its original shape during melting. The graphite structure did not clearly exhibit all five transitions in the solidification rate, contrary to observations in ground experiments. These results will be related in a quantitative way to the sulfur content as a function of position in the rod when the measurements are available.

T. LUYENDIJK
H. NIESWAAG
W. H. M. ALSEM
Department of Metallurgy,
Delft University of Technology,
NL-Delft 8, Netherlands

References and Notes

1. T. Luyendijk and H. Nieswaag, in *Proceedings of the 3rd European Symposium on Materials Science in Space* (ESA-SP 142, European Space Agency, Paris, 1979), p. 115.
2. H. Sprenger, E. Erben, H. Zeilinger, K. Schweitzer, in *ibid.*, p. 101.
3. This research was supported in part by the Dutch Department of Wetenschapsbeleid of the State Department of Economische Zaken.

27 March 1984; accepted 6 June 1984

Tribology Experiment in Zero Gravity

Abstract. *A tribology experiment in zero gravity was performed during the orbital flight of Spacelab 1 to study the motion of liquid lubricants over solid surfaces. The absence of a significant gravitational force facilitates studies of the motion of liquid lubricants over solid surfaces as controlled by interfacial and capillary forces. Observations were made of phenomena associated with the liquid on one solid surface and also with the liquid between a pair of closely spaced surfaces. Typical photographic records obtained on Spacelab 1 are described.*

The tribology experiment consisted of two parts, which were performed with separate experimental hardware and were designed to focus on different aspects of fluid-solid interactions. One part, referred to as the fluid wetting and spreading (FWS) study, was concerned with the motion of a drop of liquid lubricant on a solid surface under the influence of interfacial forces. The other part dealt with the morphology of a two-phase film under shearing between the surfaces and is referred to as the journal bearing study because journal bearing–like devices were used to carry out the studies.

Fluid wetting and spreading. Although the tertiary equilibrium among gas, fluid, and solid phases is suitably described by the well-known formula of Young (*1*), the spreading process is inherently not an equilibrium phenomenon. The low-gravity conditions during the flight of Spacelab 1 provided a unique opportunity to observe the kinetics of wetting and spreading. In the FWS study, the combined influences of lubricant properties, surface chemistry, and topography were examined.

The FWS module is a mechanized fluid-dispensing device. A separate unit is used for each of four selected test fluids. Each module contains three geometrically identical surface specimens. Twelve fluid-surface combinations were used during the Spacelab 1 flight (*2*).

The study was conducted by photographing the wetting and spreading process as soon as the test fluid "surfaces" on the solid specimen. In each test sequence, approximately 24 μl of the test fluid was displaced through the central hole of each solid specimen. Filming started at 24 frames per second for 8 seconds, then changed to 1 frame per second for 8 minutes. All solid specimens were made of 440C stainless steel with various finishing and treatment conditions as indicated in (*2*). An oblique mirror beside each specimen showed the side profile.

Cinematographic records of wetting and spreading of SRG-10 oil were analyzed by measuring the mean radius of the wetted spot at various times. Three phenomenological regimes were revealed by the spreading history:

1) Radius of each wetted spot grew to 0.15 cm in about 0.08 second with the same rate on all three specimens.

2) The wet radius on the barrier film–coated specimen grew to 0.2 cm at the end of 0.8 second. The side profile was roughly hemispheric. Wet radii on the other two specimens increased to 0.3 cm in the same period.

3) The wet radius on the barrier film–coated specimen stopped changing. Spreading continued on the other two specimens, with the wet radii reaching 0.50 and 0.38 cm, respectively, on the prewetted and clean specimens in 440 seconds. The spot shape on the prewetted specimen became oblong. A milli-*g* acceleration disturbance in this period has been established.

These results suggest that SRG-10 tends to wet and spread on a clean solid surface similar to 440C stainless steel, that the rate of advance of the contact line on a clean surface is very slow, and that barrier film coating can effectively prevent migration of the oil. Analysis of other FWS records is under way with the aid of a microdensitometer at Goddard Space Flight Center.

Journal bearing. In the normal functioning of an oil-lubricated journal bearing, the clearance space is only partially filled. On the unloaded side of the journal, natural drainage leaves behind a two-phase film which is connected to an outboard void space. Stable operation of a liquid-lubricated journal bearing is known to be dependent on the presence of the two-phase film. A series of journal bearing studies were performed on Spacelab 1 to examine the two-phase film in the capillary space of the journal bearing.

The journal bearing module has a symmetrical, rigid rotor supported by a pair of experimental journal bearings. Three bearing configurations were used to control various kinematic and geometric parameters. In the first configuration, the bearings were of plain cylindrical geometry, and the rotor could be fitted with an unbalanced mass to yield an acceleration of 0.77 *g*. In the second, the bearings were shaped by three centrally preloaded arcs. In the third, the bearings were similar to those in the first configuration, but one end of the shaft was also fitted with a ball bearing to fix the operating eccentricity to three-fourths of the radial clearance at that end.